Article

Short-Term Charging Load Prediction of Electric Vehicles with Dynamic Traffic Information Based on a Support Vector Machine

Qipei Zhang *, Jixiang Lu, Wenteng Kuang, Lin Wu and Zhaohui Wang

NARI Technology Co., Ltd., No 19 Chengxin Avenue, Jiangning District, Nanjing 211106, China;
lujixiang@sgepri.sgcc.com.cn (J.L.); kuangwenteng@sgepri.sgcc.com.cn (W.K.); wulin3@sgepri.sgcc.com.cn (L.W.);
wangzhaohui1@sgepri.sgcc.com.cn (Z.W.)
* Correspondence: zhangqipei@sgepri.sgcc.com.cn

Abstract: This study proposes a charging demand forecasting model for electric vehicles (EVs) that takes into consideration the characteristics of EVs with transportation and mobile load. The model utilizes traffic information to evaluate the influence of traffic systems on driving and charging behavior, specifically focusing on the characteristics of EVs with transportation and mobile load. Additionally, it evaluates the effect of widespread charging on the distribution network. An urban traffic network model is constructed based on the multi-intersection features, and a traffic network–distribution network interaction model is determined according to the size of the urban road network. Type classification simplifies the charging and discharging characteristics of EVs, enabling efficient aggregation of EVs. The authors have built a singular EV transportation model and an EV charging queue model is established. The EV charging demand is forecasted and then used as an input in the support vector machine (SVM) model. The final projection value for EV charging load is determined by taking into account many influencing elements. Compared to the real load, the proposed method's feasibility and effectiveness are confirmed.

Keywords: electric vehicle; support vector machine; traffic information; charging load forecast; distribution network

1. Introduction

At present, due to the increasing environmental pollution issues, there is a growing focus on minimizing the utilization of fossil fuels and reducing CO_2 emissions. The electric vehicle (EV) is clean and efficient, making it appropriate for future energy needs and sustainable development of power systems and transportation systems [1]. As EVs become more widely promoted and used globally, they are increasingly being connected to the power grid for charging purposes [2]. This connection has a significant impact on the safe operation of the power grid system and the development of the communication system [3,4]. However, with the large-scale promotion and application of various countries, EVs, as a special mobile load, are connected to the power system in large numbers for charging interaction, which brings a significant impact on the safe operation of the power system and the development of the transportation system [5]. At the same time, EVs contain an energy storage battery unit, and using a large number of EVs as energy storage units to provide auxiliary services for the power grid has also been widely studied. Accurate load prediction of EV charging load is carried out to lay the foundation for EVs to participate in the auxiliary service of power grids [6]. Therefore, effective measures should be taken to model and predict the temporal and spatial distribution of EV charging load and evaluate its impact on the distribution network [7].

In ref [8] author compared the prediction performance of random forest and the artificial neural network on EV charging load at different spatial levels, and the results showed that in the operation of a large number of EVs, aggregate prediction was more accurate than that of single charging piles. A comprehensive data-driven evaluation model

was established in [9] to study the energy use (kWh) patterns and charging load (kW) profiles of city-scale EV fleets. EVs are divided into four types: private cars, taxis, rental cars and commercial cars. The peak power consumption of different types of EVs is analyzed. Although the above model can effectively predict the load distribution of EV charging, the settings of parameters such as vehicle charging time and charging position are fixed by default, ignoring the driving dynamic characteristics of EVs.

The dynamic characteristics of electric vehicles (EVs) when carrying loads are impacted by the configuration of the road network, the selected driving route, and traffic congestion. Therefore, in order to accurately reproduce the unpredictable movement patterns of electric vehicles (EVs), it is crucial to incorporate an analysis of components associated with communication information. In ref [10] calculate actual demand for adjusting the electric network, establish an EV dynamic model using Agent-cellular automata, and enhance the micro traffic simulation model to replicate the constant change in EV charging load by integrating the traffic and charging demands of EVs. However, this model does not account for the impact of traffic information on EV route planning. Author name [11,12] took into account the interaction of traffic information and power grid information in EV driving. They created charging navigation plans for EV owners, forecasted the charging demand at each charging station, and assessed the effects of fast charging on the power grid and road network. However, this method used a fixed traffic model and did not account for the real-time dynamic features of traffic data. Author name [13] further established the "vehicle–network–road" interaction model by focusing on dynamic traffic characteristics. The model utilized the "speed-flow" BPR model to illustrate the time-varying nature of the road network and examined the spatial and temporal distribution of charging load from various vehicle types and its impact on the power flow of the distribution network. The BPR road network model was primarily used for modelling the high-speed road network. For urban roads, the delay effect of intersection impedance is not considered.

Weather conditions are significant aspects that must be included in EV charging load predictions, as they might effect EV users' travel behavior. In [14], a variety of characteristic machine learning algorithms and deep learning algorithms were applied to forecast the charging load distribution of EVs. This study used real data from the Spanish power system and accounted for the impact of the seasonal climate on EV trips. In ref [15], authors consider the long-term planning and optimization problem of en route charging station locations and charging duration to optimize passengers' waiting time and operation and capital costs while addressing the weather-induced stochasticity of ridership and the battery performance of the battery-electric buses (BEBs). In ref [16], authors use the GPS track data set to analyze the seasonal variation in charging demand for private electric vehicles in North China. And used the classical p-median model to deploy charging facilities with the charging demands in the four seasons, considering the modifiable area unit problem (MAUP) to further explore how the seasonal variance in charging demand may influence infrastructure deployment.

At present, there are two primary approaches to predicting the load of EV charging. The first method involves analyzing the impact of EV travel and charging conditions through modelling. The second method utilizes machine learning to study the influence of climate and other factors based on historical data, without specifically modelling EV operations. Nevertheless, this alternative approach has limited practicality. Moreover, there is a deficiency in the prediction of EV charging demand that takes into account road network characteristics, EV travel planning aspects, weather considerations, and power system operation factors.

In summary, this paper comprehensively considers the travel characteristics of electric vehicles and the impact of environmental factors and traffic factors on the charging load of electric vehicles. A charging demand forecasting model of electric vehicles based on the support vector machine (SVM) is proposed, and the impact of large-scale charging on the distribution network is analyzed. The main contributions of this paper are as follows.

(1) The urban road topology model is established according to the characteristics of the urban road network, and a matching distributed network model is established by using IEEE-33 nodes for the scale of the urban road network, so as to realize the coupling of the vehicle network and road network operation.

(2) By introducing the OD matrix analysis method and mmc queuing theory, the operation characteristics of a single electric vehicle are simulated in detail, and the realistic factors affecting the charging load of electric vehicles are fully considered.

(3) The predicted value of the EV road network collaborative model is imported into a SVM as historical data for prediction analysis. Considering the weather-sensitive factors, emergencies and random factors of EVs, the particle swarm optimization algorithm is used to optimize the short-term prediction load of EVs, and the influence of large-scale EV charging on the node voltage and network loss of the distribution network is evaluated.

2. EV Charging Load Forecasting Model Based on Traffic Information

EVs have the characteristics of both vehicles and mobile loads. The traffic demand, travel distribution and path planning in the travel process will be affected by traffic information such as road structure and road congestion, and their charging behavior and charging demand will affect the load distribution, node voltage and network loss of the distribution network [17,18]. Therefore, the accurate prediction of EV charging load needs to integrate the traffic network with the distribution network, and combine the traffic network with the distribution network to accurately characterize the impact of EVs' spatial and temporal changes on the power system.

2.1. Model Assumption

EV travel in a city has been defined by a complex energy consumption process. This study proposes the following assumptions regarding the EV charging load model in order to achieve an optimal balance between precise EV charging and discharging load forecast and efficient EV travel simulation.

(a) Considering the uncertainty of the complex situation of urban roads, the road impedance coefficient can be used to characterize EV driving on the road, assuming that the road congestion situation follows the daily traffic peak and trough periods.

(b) Considering the wide variety of electric vehicle (EV) types, it is challenging to articulate their individual operating characteristics. This work assumes certain operating load conditions for electric vehicle (EV) monomers, examines the shared characteristics of EV travel, categorizes EVs based on their kind, simplifies the charging and discharging properties of monomer EVs, and achieves efficient polymerization of regional EVs.

(c) Considering the coupling distribution between the distribution network nodes and the actual traffic network, it is assumed that all load nodes in the 33-node distribution network can correspond to the traffic nodes.

2.2. The Traffic Network Model

The traffic network is the basis for vehicle driving and charging. Therefore, in order to quantitatively describe the road structure, the graph theory method is used to abstract the actual road network and establish a traffic network model. The topological structure of the traffic network is shown in Figure 1.
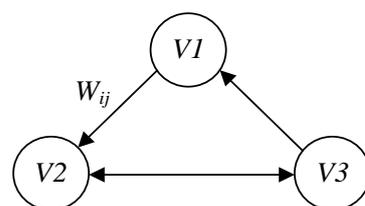
Figure 1. Topological structure of the traffic network.

As shown in Figure 1, the two-way arrow is the two-way road, and the one-way arrow is the one-way road. The mathematical model of traffic network is constructed based on the topology of traffic network.

$$
\begin{cases}
G^{\mathrm{T}} = (V, E, K, W) \\
V = \{v_i \mid i = 1, 2, 3, \cdots, n\} \\
E = \{v_{ij} \mid v_i \in V, v_j \in V, i \neq j\} \\
K = \{k \mid k = 1, 2, 3, \cdots, m\} \\
W = \{w_{ij}^k \mid v_{ij} \in E, k \in K\}
\end{cases}
\tag{1}
$$

where G^{T} is the traffic network. V represents the set of all nodes in G; v_{ij} represents the road from road node i to road node j. E is the set of all road sections of the network G^{T}; K denotes the set of time periods divided, that is, the whole day is divided into m time periods. W is the set of road weights, represents the road resistance, indicating the travel cost of the road section, which can be quantified by time, speed and travel cost.

The analysis of EV charging load focuses mostly on the city's interior roads, which exhibit dynamic and variable characteristics with multiple intersections in the urban road network. Therefore, this paper divides the composition of urban roads into nodes and road sections. The node impedance and road section impedance represent the congestion degree of traffic lights at intersections and the traffic congestion degree of road sections, respectively. The road is divided into smooth ($0 < S \leq 0.6$), slow ($0.6 < S \leq 0.8$), crowded ($0.8 < S \leq 1.0$) and severe congestion ($1.0 < S \leq 2.0$) by saturation variable S. According to the traffic network congestion, the road section impedance and node impedance models corresponding to different saturation variables S are constructed.

2.2.1. The Traffic Road Impedance Model

$$
R_{v_{ij}}(t) = \begin{cases}
R_{v_{ij}}^1(t) : t_0\left(1 + \alpha(S)^\beta\right), 0 \leq S \leq 1.0 \\
R_{v_{ij}}^2(t) : t_0\left(1 + \alpha(2 - S)^\beta\right), 1.0 < S \leq 2.0
\end{cases}
\tag{2}
$$

where $S = M/C$ and M represents road traffic flow. C is the current road capacity. t_0 is the travel time of EV through the whole road when the flow is zero. α and β are impedance influence factors. The $R_{v_{ij}}(t)$ calculated by Formula (2) represents the impedance coefficient of each traffic road under different traffic impedances, and represents the speed of EV driving on this road.

2.2.2. The Traffic Nod Impedance Model

$$
C_{v_i}(t) = \begin{cases}
C_{v_i}^1(t) : \dfrac{9}{10}\left[\dfrac{c(1-\lambda)^2}{2(1-\lambda S)} + \dfrac{S^2}{2q(1-S)}\right], 0 < S \leq 0.6 \\
C_{v_i}^1(t) : \dfrac{c(1-\lambda)^2}{2(1-\lambda S)} + \dfrac{1.5(S-0.6)}{1-S}S, S > 0.6
\end{cases}
\tag{3}
$$

where $C_{v_i}(t)$ is the conversion period of traffic lights in period t. v_i represents traffic node i. λ is the proportion of green light signal. q is the vehicle arrival rate of the road section. Therefore, the model of urban road impedance can be expressed as the sum of node impedance and road impedance. It can be expressed as:

$$
W_{ij}^k(t) = C_{v_i}(t) + R_{v_{ij}}(t)
\tag{4}
$$

2.3. The Distribution Network Model

The grid–transportation network vehicle–network integration model achieves node connection between the distribution network and the road network in space. Thus, it

is essential to create a distribution network of a specific scale that aligns with the road network concept.

$$\begin{cases} G^D = \left(V^D, E^D, \psi^D\right) \\ V^D = \{n_i \mid i = 1, 2, 3, \cdots, n_G\} \\ E^D = \left\{(n_i, n_j) \mid n_i, n_j \in V^D\right\} \\ \psi^D = \left\{(r_i, x_i, c_i, P_i,) \mid (n_i, n_j) \in E^D\right\} \\ B^D = \{(P_i, Q_i) \mid i = 1, 2, 3, \cdots, n_G\} \\ F^D = \{f_i(t) \mid t = 1, 2, 3, \cdots, T\} \end{cases} \tag{5}$$

where V^D represents the node set of the distribution network. n_i, n_j represent nodes i and j in the road network. E^D is the branch set of the distribution network. ψ^D is the basic parameter set of the distribution network; B^D is the average active power and reactive power of each node. F^D is the load variation coefficient between nodes. n_G is the number of nodes in the distribution network.

The total load of different nodes is the accumulation of the basic load of the grid node and the charging power of the electric vehicle at the access node.

$$P_n = P_{n,f} + \sum_{i=1}^{N} P_{i,t} \tag{6}$$

where P_n represents the total load of the node n. $P_{n,f}$ denotes the base load of the n th node. N denotes the total number of charging vehicles in the t period of the i th node. $P_{i,t}$ denotes the charging power of the i th vehicle during the t period. Constraint (6) ensures the power balance of each node in the distribution network node.

2.4. EV Operation Model

Combined with the actual development of electric vehicles in China, electric vehicles can be divided into three types, as shown in Table 1. Detailed operating parameters of electric vehicles are shown in Table A3 in Appendix C.

Table 1. Type of electric vehicle.

EV Types	Operational Performance	Charging Type
Private vehicles	fixed	slow charge
Taxi	nonstationary	fast charge
Other public vehicles	nonstationary	slow/fast charge

Based on EV classification, in order to analyze the distribution characteristics of EV all-day travel, the OD origin–destination matrix method is introduced to construct the EV monomer operation model. The starting and ending matrices of EVs are deduced by the change in traffic flow in each period of the road section.

$$\begin{cases} min \quad F = \sum_{a=1}^{r} \left(\sum_{i=1}^{m} \sum_{j=1}^{m} T_{ij} A_{a\_ij} - Q_a\right)^2 \\ \text{s.t.} \quad T_{ij} \geqslant 0 \forall i, j \end{cases} \tag{7}$$

where Q_a is the actual traffic flow of road a. r is the number of road sections. m is the total number of road nodes. T_{ij} is the element in the OD matrix to be solved [19,20]. A_{a_ij} is the probability of passing through section a for vehicles departing from point i to point j. In this paper, the nonequilibrium OD backstepping model is used; A_{a_ij} is a constant and unrelated to the road traffic flow. The constraint in (7) indicates that the overall traveling time of EV cannot be less than 0.

Based on the method mentioned above, the OD matrix B of three types of EV for 24 h a day is obtained. The matrix B consists of 72 sub-matrices $B_{m \times m}^{T, T+1}$, which represents the OD

matrix of three types of electric vehicles in the $T \sim T+1$ period. The OD travel probability matrix $C_{m \times m}^{T,T+1}$ of the three electric vehicles at each time of the day can be obtained by:

$$c_{ij}^{T,T+1} = \frac{b_{ij}^{T,T+1}}{\sum_{j=1}^{m} b_{ij}^{T,T+1}} 1 \leqslant i, j \leqslant m \tag{8}$$

where the molecule represents the number of electric vehicles arriving at the road network node j from the road network node i at the time of $T \sim T+1$. The denominator represents the total number of electric vehicles starting from the road network node i; when $i = j$, $c_{ij}^{T,T+1}$ is the probability that there is no travel demand for electric vehicles during this period of time. $b_{ij}^{T,T+1}$ is the OD matrix of three types of electric vehicles in the $T \sim T+1$ period, which is in matrix B.

Various criteria are established to determine the charging status for different types of EVs. At time t, the remaining electric charge of the EV can be denoted as Cr_t.

$$Cr_t = Cr_{t-1} - \Delta l \cdot \Delta Cr \tag{9}$$

where Δl is the travel distance from time $t-1$ to time t. Cr is the EV power consumption of 100 km. When the battery power of the electric vehicle at time t meets the following characteristics, a fast charging demand is generated.

(1)   Private car

The parking time is long, and the charging method can be selected independently. If the battery power is less than 10%, it will cause damage to the battery. During the driving process, the owner determines that the battery power after reaching the destination is less than 10% of the total battery capacity ST.

$$Cr_t \leqslant ST \tag{10}$$

(2)   Taxi

The parking time is short, and only fast charging can be selected to supplement the electric energy. When the remaining power at time t is lower than the set threshold power Cr_C, the fast charging demand is generated. The SOC corresponding to the threshold power is set to be 0.25.

$$Cr_t \leqslant Cr_C \tag{11}$$

(3)   Other public vehicles

It is assumed that the battery power is lower than the threshold power Cr_C when the fast charging demand is generated, and the threshold power setting is the same as the taxi.

The Monte Carlo method is used to simulate the initial travel time t s, initial operating power Cr_0 and initial position O_i of three types of electric vehicles in a day. Combined with the OD matrix, the spatial and temporal distribution of EV charging demand is analyzed. The random sampling method is used to generate the destination D_j information at time t. Assuming that the driver chooses the shortest path to the destination D_j, the shortest path set R between O_i and D_j is obtained by the Dijkstra shortest path algorithm, and the distance l_{OD} of each section is obtained by the road network topology matrix. Assuming that there are s sections in the set R, the speed $V_{(t)}$ on the hth section is calculated by using the improved speed flow model. The driving time ΔT_h of the section is:

$$\Delta T_h = \frac{d_h}{V_h(t)} \tag{12}$$

Then, the total travel time from O_i to D_j shows as Equation (13), representing the sum of the time taken by the EV to travel all the road sections.

$$\Delta T_{ij} = \sum_{h=1}^{S} \Delta T_h \tag{13}$$

Firstly, according to the above Formula (9), the battery capacity Cr_t when passing through the road section h is calculated. If the fast charging condition defined above is satisfied, the fast charging demand is generated. The travel time ΔT_{ij} is used to obtain the time T to reach the destination D_j. $D_j D_j$ is used as a new initial O_j, and the corresponding OD probability matrix at time T is called. The driving trajectory of electric vehicles in a day is simulated in turn, and the spatial and temporal distribution of 24 h fast charging demand in a day is finally obtained.

When EV arrives at the charging pile for charging, it may need to queue. This paper refers to the mmc queuing theory to calculate the queuing time of EV charging. If the arrival process of the vehicle to each charging station obeys the Poisson distribution, and the number of charging requirements for the service to the charging station per hour is taken as the parameter λ, the average queuing waiting time W_q of the system is

$$W_q = \frac{(c\rho)^c \rho}{c!(1-\rho)^2 \lambda} P_0 \tag{14}$$

$$P_0 = \left[\sum_{k=0}^{c-1} \frac{1}{k!} \left(\frac{\lambda}{\mu} \right)^k + \frac{1}{c!} \cdot \frac{1}{1-\rho} \cdot \left(\frac{\lambda}{\mu} \right)^c \right]^{-1} \tag{15}$$

$$\rho = \frac{\lambda}{c\mu} \tag{16}$$

The average charging queue length L_s of EV is

$$L_s = \frac{(c\rho)^c \rho}{c!(1-\rho)^2} P_0 + \frac{\lambda}{\mu} \tag{17}$$

where c is the number of chargers in the charging station. μ is the number of vehicles completed per unit time service for each charger, and the P_0 represents the charging time for electric vehicles. ρ is the service strength of the charger. Constraint (17) considers the average charging vehicle and charging time of the charging station, and obtains the average EV charging amount of each charging node.

Finally, the charging demand model is judged. When the charging demand is triggered, the corresponding destination slow charging or charging station fast charging is carried out. The total load of the node is obtained by superimposing the charging demand load of each node with the basic load. Parameters such as EV charging load peak, charging load peak and valley period, and EV charging load demand are recorded.

3. Multi-Factor EV Charging Load Forecasting Model Based on SVM

A SVM has been extended to solve the problem of nonlinear regression estimation, and compared with the neural network method, it has significant advantages. It is considered as an alternative method of the artificial neural network method, and has become a research hotspot and focus in the field of machine learning [21]. On the one hand, the change in EV load has its uncertainty, such as the change in the travel peak period, the change in weather, and the occurrence of accidents, which cause the random interference of EV charging load. On the other hand, under certain conditions, EV load changes regularly according to a certain trend. Therefore, in the short-term load forecasting of EV charging load, it is necessary to fully analyze, master and utilize its regularity, and take into account the influence of various factors. The following takes the climate data of a certain area in Zhejiang Province of China as an example to analyze and summarize the periodic law of load and various influencing factors of prediction. Considering and utilizing these

characteristics of the load, a more realistic prediction model can be established to improve the prediction accuracy.

3.1. EV Short-Term Load Characteristic Component Analysis

The short-term charging load of EV can be divided into the following components:

(1) EV charging load forecasting components

EV charging load forecasting components is the predicted charging load based on the simulation analysis of EV example based on the road network, which is mainly determined by the parameters of the road network and the distribution network. In this paper, the predicted value of EV charging load based on the analysis of traffic network is taken into account as a component.

(2) Typical load components of EVs

The load component of EVs is primarily influenced by the distinctive charging and operating characteristics of each EV, which are determined by the kind of EV and the distribution of different EV types. The variations in these two components of EV clusters, made up of multiple EVs, determine their fundamental charging load characteristics and distinct reactions to numerous influencing factors, displaying diverse response characteristics.

(3) Weather-sensitive component of EVs

Weather-sensitive components are primarily affected by weather conditions like temperature, visibility, rainfall probability, and other related aspects [22]. Various weather conditions will influence the transportation decisions of electric vehicle users.

(4) Anomalous or special event load component

Abnormal and special events like system failure, power constraints, and natural disasters greatly affect the load. These events exhibit high levels of unpredictability and are challenging to forecast. They can only be evaluated based on the experience of dispatchers. It can be enhanced through manual rectification or an expert system.

(5) Random component of EV

The sequence of EV charging load exhibits significant volatility because of the unpredictability of user psychology. The stochastic element of the charging load is the portion of the load that cannot be accounted for and may be incorporated into the model or the algorithm.

Therefore, the total load of the EV charging system can be expressed as follows:

$$Y(t) = For(t) + Nor(t) + Wea(t) + Spe(t) + Ran(t) \tag{18}$$

where $Y(t)$ represents the total load. $For(t)$ is the EV charging load forecasting components. $Nor(t)$ represents typical load components. $Wea(t)$ is the weather-sensitive component. $Spe(t)$ represents the weight of special events. $Ran(t)$ represents the random load component.

3.2. The Data Preprocessing Process

Short-term load forecasting for EVs requires integration with EV simulation forecasting data and a substantial amount of historical data for analysis. Historical data collection and analysis can be influenced by objective factors like measurement equipment and data transmission, as well as subjective factors like artificial manipulation and power limitations. This can result in missing, inaccurate, or abnormal data in historical load data, commonly referred to as bad data. Data preprocessing involves cleaning historical load data by removing irregular data, filling missing data, and filtering out poor data to enhance the accuracy of load forecasts.

(1)   Missing data processing.

Linear interpolation is utilized to fill in missing data when the temporal interval is not significant. For instance, if the load value of time n, $n + 1$: f_n and f_{n+1} are given, and there are no intermediate data, the value of the intermediate time $n + j$ can be calculated.

$$f_{n+j} = f_n + \frac{f_{n+1} - f_n}{i} \cdot j, 0 < j < i \tag{19}$$

For significant time intervals, linear interpolation may not be optimal, and data from neighboring days are utilized instead. Due to significant variations in load data among different day kinds, it is essential to use data from the same date type when correcting the data.

(2)   Error data processing.

The load at a specific point is compared with the load values immediately preceding and following it. If the discrepancy exceeds a specific threshold, meaning the load data range is beyond ±10% of the load value before and after it, horizontal processing is utilized. The current load value is compared with the load values from the same time on the previous day and two days prior. Vertical processing is used if the variation exceeds ± 10%. The two methods are as follows:

Due to the cyclical nature of electricity load, different dates, particularly those before and following, are expected to exhibit similar load patterns. It is important to keep the load value within a specific range and fix any data that fall beyond this range.

$$\begin{cases} y(d,t) = \begin{cases} \overline{y(t)} + \theta & y(d,t) > \overline{y(t)} \\ \overline{y(t)} - \theta & y(d,t) < \overline{y(t)} \end{cases} \\ \left| y(d,t) - \overline{y(t)} \right| > \theta \end{cases} \tag{20}$$

where $y(d,t)$ is the load value at the time t of the day d. $\overline{y(t)}$ is the average value of the load at the same time of the data to be processed in recent days.

3.3. The Selection and Normalization of Input Variables and Samples

The analysis of load characteristics indicates that EV charging load is influenced by EV type, the urban road network, season, weather, and other factors. Extensive statistical investigation indicates that temperature and rainfall likelihood are the weather conditions that have the most significant influence on EV charging load. This research takes into account the impact of EV type, rainfall probability, and temperature on charging load when developing the forecast model. The impact of a specific order of magnitude of the characteristic index on the categorization may be emphasized during the operation process due to differences in dimension and order of magnitude. To remove the impact of varying characteristic index units and orders of magnitude, standardization is required to ensure each index value is normalized within a consistent numerical range.

(1)   Normalization of EV charging load data

The load is processed logarithmically as:

$$x'_{ij} = \lg(x_{ij}) \tag{21}$$

where x_{ij} is the original load and x'_{ij} is the normalized load.

(2)   Normalization of temperature data

The normalization formula used in this paper is:

$$T'_{ij} = \left(T_{ij} - T_{jmin} \right) / \left(T_{jmax} - T_{jmin} \right), i = 1, 2, \ldots, n; j = 1, 2, \ldots, m \tag{22}$$

where T_{ij} is the original temperature °C. T_{jmin} and T_{jmax} are the minimum and maximum values in $T_{1j}, T_{2j}, \cdots, T_{nj}$; T'_{ij} is the normalized temperature coefficient.

(3)   Normalization of rainfall probability

The rainfall probability factor is reduced to a value between [0–1]. In this way, each datum is linearly transformed to the value range of [0–1], and is a dimensionless quantity with the same scale. Finally, the output training, test and prediction data are denormalized and restored to the actual value by reduction calculation.

3.4. Selection of the Kernel Function

Commonly used kernel functions are: the linear kernel function, the polynomial kernel function, the radial basis kernel function, the Sigmoid kernel function, and the Fourier kernel function. For the regression estimation of the data of different system processes, there is a corresponding kernel function with the best effect. The radial basis function has the following advantages:

(a)   The representation is simple, even for multivariate input does not increase too much complexity;
(b)   Radial symmetry, good smoothness, any order derivative exists;
(c)   Because the function is simple and has good analyticity, it is convenient for theoretical analysis.

Based on these characteristics of the radial basis function, this paper uses the radial basis function as the kernel function in the regression model.

The specific forms are as follows:

$$K(x, x_i) = \exp\left(- \| x - x_i \|^2 / \sigma^2\right) \tag{23}$$

where x represents the dimension input vector of m dimension. x_i is the center of the i th radial basis function, and has the same dimension with x. σ is the standardized parameter and determines the width of the function around the center point; $\| x - x_i \|$ is the norm of the vector $x - x_i$ and represents the distance between x and x_i.

The radial basis function transforms the sample data nonlinearly into a high-dimensional space, which can deal with the situation where the input and output are nonlinear. When taking a specific range of parameters, its performance includes a linear kernel function and a Sigmoid kernel function, that is, they belong to the radial basis function in special cases. In addition, the representation is simple, only one parameter needs to be adjusted, any order derivative exists, and there is radial symmetry, good smoothness, and good analyticity, and the multivariate input does not increase the complexity too much, so it is convenient for theoretical analysis.

3.5. Establishment of the SVM Model

The specific process of the improved particle swarm optimization algorithm is as follows: on the premise of ensuring the uniform distribution of the initial population, the basic operation of the standard particle swarm optimization algorithm is first run until the particle is judged to fall into the premature state, and then the particle solution space is redistributed, so as to guide the particle to jump out of the local optimum quickly and accelerate the convergence. The specific algorithm and process are as Figure 2:

The error evaluation of this paper "take" the root mean square relative error (MSE) as the index, and the specific error analysis is as follows

$$E_{MSE} = \sqrt{\frac{1}{n} \sum_{i=1}^{n} \left(\frac{L_i - \hat{L}_i}{L_i}\right)^2} \times 100\% \tag{24}$$

where L_i and $\hat{L}_i$ are the actual load and the predicted load. n is the number of load data. In power load forecasting, the average relative error MAPE and the root mean square relative error MSE are often used as the evaluation criteria for errors.
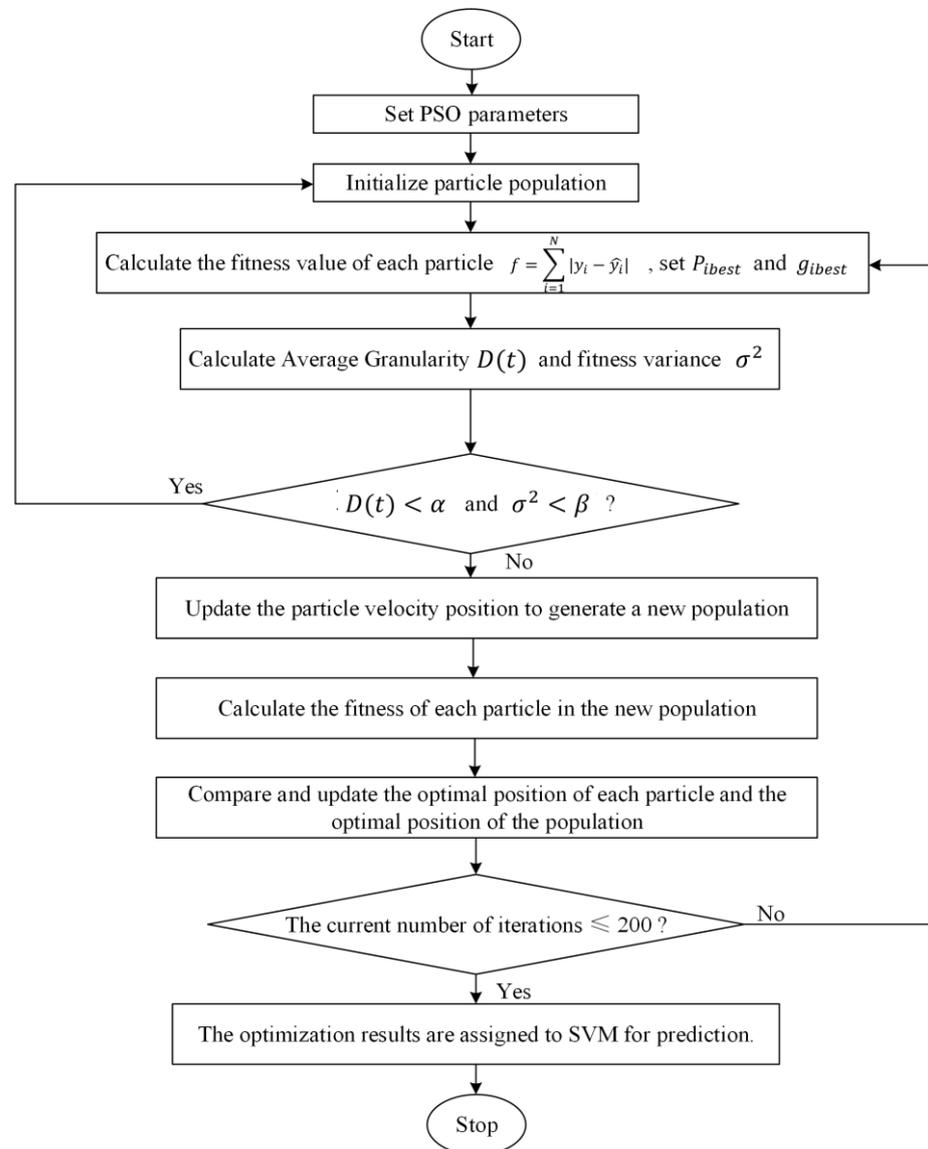
Figure 2. Specific algorithm and process of EV charging load prediction.

4. Example Analysis and Result Discussion

Taking EV operation path planning as the center, the spatial and temporal distribution of electric vehicle charging demand load is predicted through specific examples. The obtained EV operation characteristics and processed historical load data are introduced into a SVM to realize the charging load prediction of electric vehicles considering multiple factors [23,24]. According to the voltage quality requirements of China's distribution network, this paper sets the safety threshold of voltage drop as 7%.

4.1. EV Charging Load Forecasting Based on Traffic Information

The simulation time is set to 24 h a day, and the vehicles with charging demand are recharged in the form of slow charging and fast charging. Figure 3 shows the spatial and temporal distribution of EVs with specific charging demand.
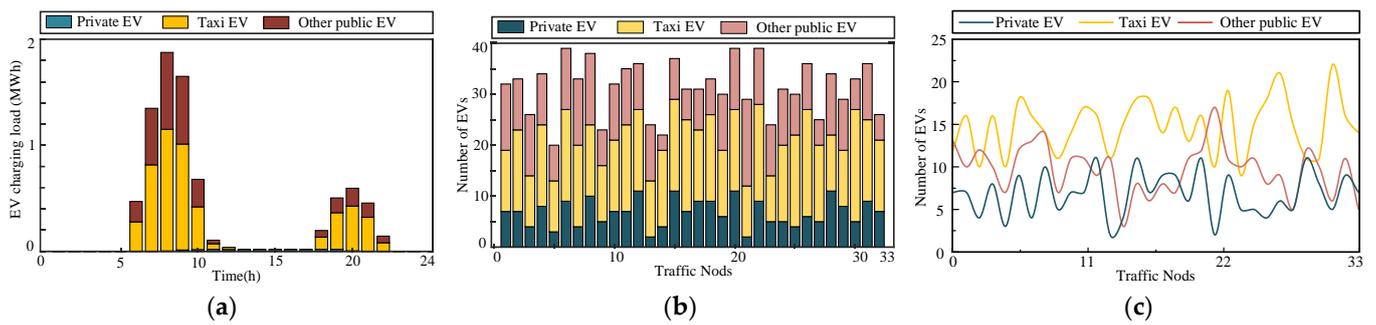
Figure 3. The spatial and temporal distribution of specific charging demand vehicles. (**a**) The time distribution of different types of electric vehicle charging load. (**b**) Spatial distribution of the overall EV operation. (**c**) Spatial distribution of different types of EV operation.

As shown in Figure 3a, it can be seen that the EV charging load is concentrated in the two periods of 6:00~11:00 and 18:00~22:00 in the morning, and the charging load is mainly taxi EVs and other public EVs, accounting for 61.18% and 36.31% of the total charging amount, respectively. The charging load of private EVs is less, accounting for only 2.5% of the total charging capacity. It can be seen that taxi travel and public car travel need frequent charging to maintain their normal operation due to their long travel time and fast charging support. The proportion of different types of EV charging power consumption is used as a prediction parameter, which is introduced into the EV charging load prediction components.

As shown in Figure 3b,c, it can be seen that the distribution of overall EVs in nodes is random, but the number of overall taxi EVs is the largest, accounting for 47.3% of the total number of EVs in the calculation steps, followed by public EVs, accounting for 31%, while the number of private EVs is the least, accounting for 21.7%. Therefore, the proportion of different EVs is also introduced into the EV charging load prediction components as a parameter to enhance the reliability of SVM multi-factor prediction. The spatial and temporal distribution of EV charging demand on distribution network nodes is shown in Figure 4.
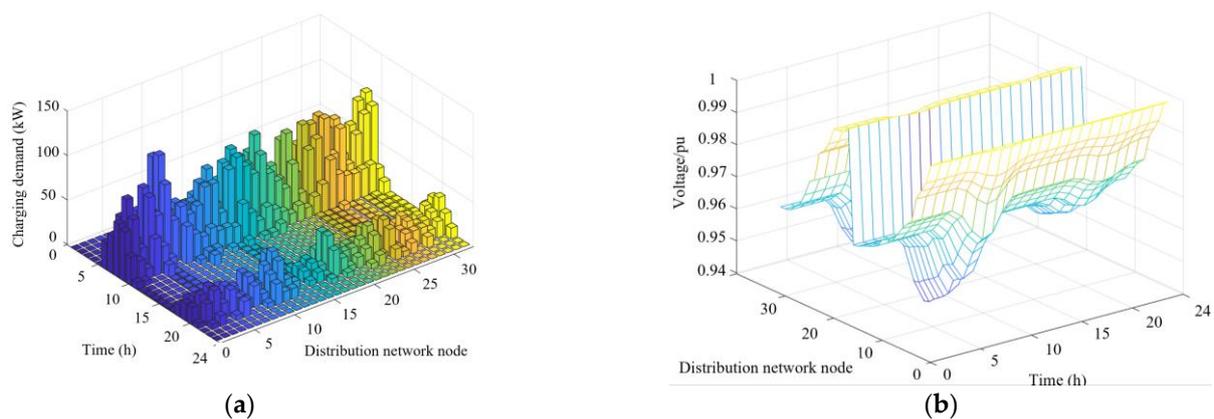
Figure 4. The spatial and temporal distribution of EV charging demand on distribution network nodes. (**a**) Variation in EV charging load in the distribution network. (**b**) Variation in node voltage change in the distribution network.

It can be seen from Figure 4a that the EV charging load of multiple nodes reaches a peak at 6:00–8:00 in the morning, and the highest node EV charging load reaches 107 kW, corresponding to the early peak charging demand. In Figure 4b, it can be seen that due to a large number of EVs accessing charging, the voltage of the distribution network node drops. Among them, the voltage curve drops the most during the 6:00–10:00 period, with a maximum drop of 5.39%, which has a certain impact on the safe operation of the

distribution network. The average voltage of distribution network nodes will produce voltage drop after EV charging load is connected, and the change in node voltage is shown in Figure 5.
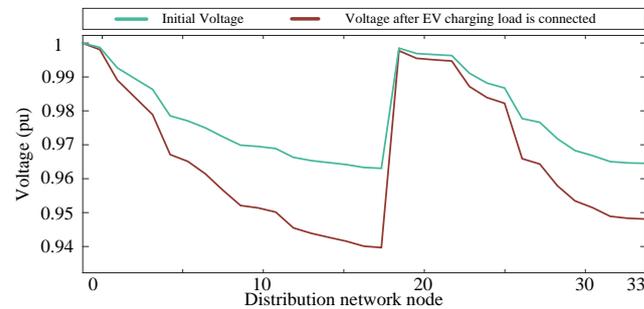
Figure 5. Variation in the average voltage of distribution network node after EV charging load is connected.

Comparing the above Figures 4b and 5, it can be seen that in Figure 4b, due to a large number of EVs accessing charging, the voltage of the distribution network node drops. Among them, the voltage curve drops the most during the 6:00–10:00 period. The drop of the distribution network node 17 is higher than that of other traffic nodes, with a drop of 6.59%. However, this paper considers the dynamic travel characteristics of EVs, and the voltage drop is less than the threshold of 7%. Similarly, at 17:00–22:00, with the increase in EV travel, the EV charging load increases, and the voltage curve also drops, but the drop does not exceed the safety threshold limit of 7%, and the distribution network maintains safe operation. The simulation parameters of EV charging and discharging operation obtained from the data set are shown in Table 2.

Table 2. EV charging load forecasting components.

Components	Value
Proportion of Private EVs	21.7%
Proportion of private EV charging load	2.51%
Proportion of taxi EVs	47.3%
Proportion of taxi EV charging load	61.18%
Proportion of other public EVs	31.0%
Proportion of other public EV charging load	36.31%
EV charging peak load	107 kW
EV charging peak period	6:00–8:00
Distribution network maximum node voltage drop	5.39%

Dynamic compensation technology is often considered to be the ultimate way to solve the problem of voltage drop. According to the different types of compensation signals and the different connection modes of dynamic power quality regulation devices, it can be divided into two modes: series voltage compensation and parallel current compensation. For distributed resources such as EVs with power consumption regularity, voltage quality control devices such as uninterruptible power supply (UPS), dynamic voltage restorer (DVR), and static synchronous compensator (DSTATCOM) can well eliminate the impact of EV charging load instantaneous access on the load.

In conclusion, by summarizing the charging load forecasting components of electric vehicles based on the traffic network in Table 3. The information from Table 3 is utilized as components for forecasting EV charging demand. It is included in the support vector machine (SVM) along with historical EV charging load data, weather variables data, and special conditions data to conduct a comprehensive prediction of EV charging load using multiple factors.

Table 3. PSO parameters.

Parameters	Value
Population m	20
Maximum number of iterations T_{max}	100
Inertia weight coefficient w	[0.4, 0.9]
Acceleration constant c_1/c_2	2/2

4.2. Multi-Factor Analysis of EV Charging Load Forecasting Based on A SVM

(1)   Determination of model parameters

When using a SVM to solve the regression estimation problem, after determining the kernel function, it is necessary to select the parameters of the Gaussian radial function σ, C and ε. These parameters have a great influence on the performance of the learning machine, but so far, there is no unified and effective theoretical guidance on how to select these parameters. For the parameters C and ε, C is too small, the sample data beyond the sample penalty ε are small, so that the training error becomes larger; if C is too large, the corresponding penalty is too large, the training error of the learning machine becomes smaller, and the promotion ability becomes worse. If ε is too small, the required regression estimation accuracy is high, but the number of support vectors increases; if it is too large, the regression estimation accuracy is reduced, the number of support vectors is small, and the sparsity of the SVM is large. For the least squares support vector machine (LS-SVM), the parameters that need to be selected are only the parameters σ and C in the kernel function, and the parameters that need to be selected are reduced, and the difficulty of selection is reduced. In this paper, the improved particle swarm optimization algorithm is used to select σ and C. The initialization of each parameter in the particle swarm optimization algorithm is as Table 3.

(2)   SVM load prediction based on particle swarm optimization

The SVM model's main parameters are predicted using the particle swarm optimization (PSO) technique. The anticipated results are then compared with the actual load data on the forecast day using the average absolute value error calculation method. To minimize the impact of random variables, many sample sets in a specific region of Nanjing, Nanjing Province in 2019 were individually forecasted and the average of the predictions was calculated. Among them, the weather data come from the MERRA-2 open source data set [25]. The EV charging load data are derived from the historical data of Nanjing, Jiangsu Province.

In order to enhance the probability of identifying the global optimal solution within the conventional particle swarm optimization technique, it is recommended to distribute the initial particle swarm throughout the entirety of the solution space as a result of the random selection procedure. However, there is a limitation on the number of particles, notwithstanding the vastness of the solution space. The probability of becoming trapped in local optima is heightened by the uneven distribution of finite particles inside the solution space. This study introduces an improved particle swarm optimization technique that integrates a repulsion mechanism subsequent to the mutual attraction and aggregation process of particle position renewal in the original algorithm. The purpose of this adjustment is to achieve a harmonious equilibrium between the forces of attraction and reciprocal repulsion observed among particles, in order to avoid early convergence. The places in the solution space are denoted as r when the distance and fitness variance between particles decrease to a certain threshold. The diversity of particle search has been significantly enhanced.

After iterative calculation, The results of SVM prediction without considering EV charging load prediction components are shown in Table 4, The SVM prediction results considering EV charging load prediction components are shown in Table 5. the parameter optimization results of the model are shown in Table 5. Figure 6 demonstrates the impact of EV transportation network simulation components on SVM prediction [26].

The comparison between the predicted load curve and the actual load curve is shown in Figure 7.
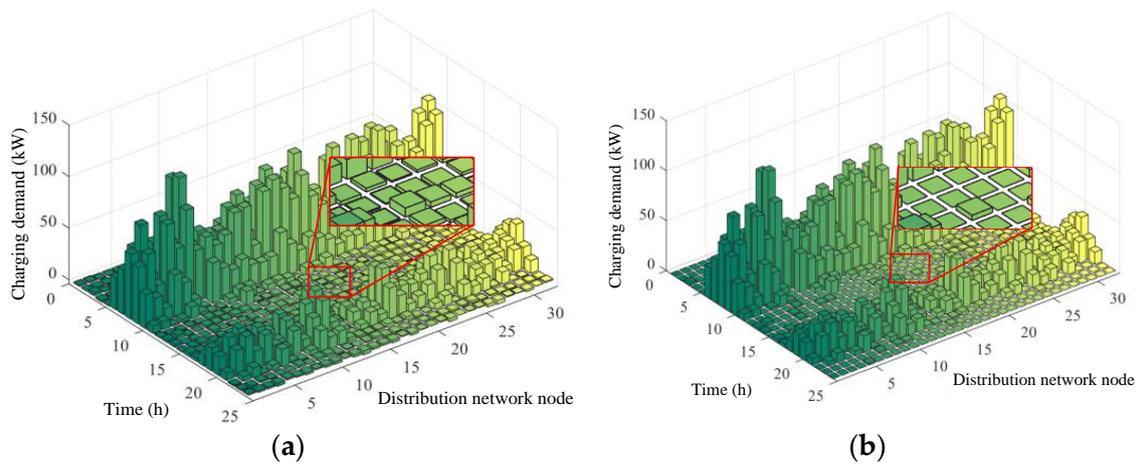
Figure 6. Influence of EV transportation network simulation components on SVM prediction. (**a**) SVM forecasting results without EV simulation components. (**b**) SVM forecasting results with EV simulation components.
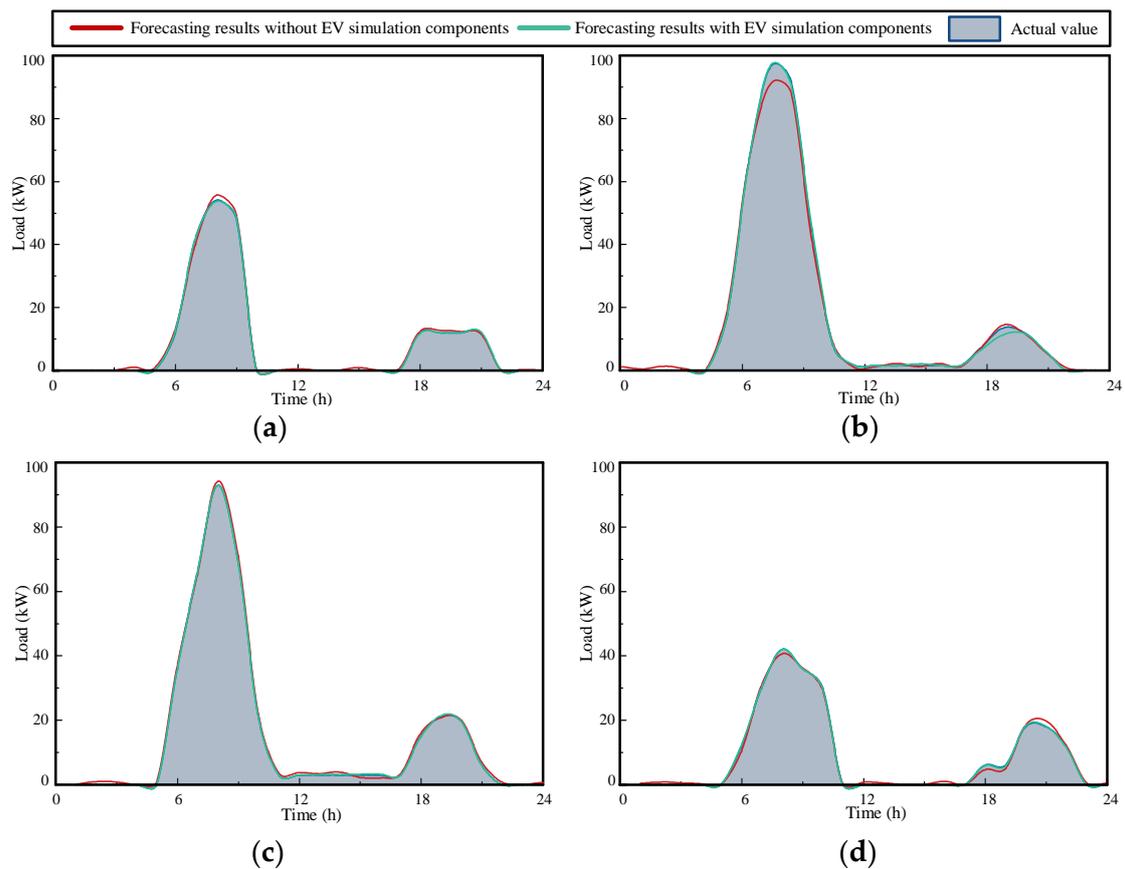
Figure 7. Actual and predicted EV charging load of typical distribution network nodes. (**a**) EV charging and discharging load prediction of distribution network node 7. (**b**) EV charging and discharging load prediction of distribution network node 12. (**c**) EV charging and discharging load prediction of distribution network node 17. (**d**) EV charging and discharging load prediction of distribution network node 20.

Table 4. SVM prediction results without considering EV charging load prediction components.

Parameters	1	2	3	4	5	...	30	31	32
Error	2.75%	2.03%	3.17%	3.35%	2.15%	...	4.00%	2.15%	2.17%
Average Error					2.72%				

Table 5. SVM prediction results considering EV charging load prediction components.

Parameters	1	2	3	4	5	...	30	31	32
Error	1.15%	1.27%	1.29%	1.57%	1.97%	...	1.35%	1.13%	1.10%
Average Error					1.65%				

Detailed SVM prediction results are shown in Table A1 (Appendix A) and Table A2 in Appendix B.

As shown in Figure 6, it can be seen that when EVs are forecast using only historical data combined with weather factors and special circumstances without considering the charging load prediction results of EV traffic network, SVM prediction results are prone to errors in some EV travel trough periods due to the uncertainty of EV travel conditions. It makes the distribution network nodes that should be zero meet the demand of EV charging at all times. After analyzing the EV traffic network charging load prediction results, taking into account the impact of EV travel duration on the charging load, the SVM prediction results are more precise. The prediction accuracy for EV charging load demand during morning and evening peaks has improved, and the charging load during off-peak travel times is more closely aligned with the actual values.

The prediction results in Tables 4 and 5 and Figure 7 show that SVM charging load prediction considering EV network operation model has higher prediction accuracy. The average absolute error of the prediction model, excluding reference nodes, is 1.24% in the 32 prediction nodes. The maximum error is less than 2.51%. The prediction error exhibits a roughly twofold reduction compared to the prediction outcomes that do not incorporate the operation of the EV traffic network. Hence, this approach is both efficient and viable for predicting the short-term charge load of EVs. The widespread use of electric vehicles (EVs) has led to the development of a convergent and flexible EV regulating system, which can effectively support the functioning of the power system. The method suggested in this research offers data support and a theoretical foundation for the inclusion of electric vehicles (EVs) in power grid auxiliary services as a distributed resource [27,28].

5. Conclusions

An integrated modelling analysis was conducted on the distribution network, the transportation network, and the vehicle network, resulting in the establishment of a dynamic traffic network model, a distribution network model, a single EV mobility model, and an EV charging queue model. A predictive model for electric car charging demand was developed and the findings were used as inputs for the SVM. Analyzing the charging load of electric vehicles involves evaluating multiple influencing factors. The conclusions are derived from the simulated example.

The established traffic network model considers the traffic Information of the urban road network and the characteristics of multi-intersection nodes, analyzes the influence of traffic information on road section impedance and node impedance, and realizes the interactive coupling of traffic information and grid information.

The OD matrix analysis method is used to simulate the mobility characteristics of EV travel. Through the interaction between traffic information and power grid information to predict the spatial and temporal distribution of charging load, it can be seen that there are obvious differences in the distribution of EV charging load in different distribution network nodes, and it is easy to superimpose with the peak load of the distribution network in time, which will affect the prediction of EV load. In this paper, the EV load forecasting

results considering traffic information and grid information are introduced into the SVM as components. Considering the influence of various additional factors, the average error between the predicted value and the actual value is only 1.65%.

This paper presents a simulation model of EV charging and discharging, which can predict different EV charging loads. In the future deployment of urban EV charging piles, it provides a basis for the expansion and planning of EV charging stations. At the same time, EV charging load prediction data influenced by multiple factors can provide support for power system day-ahead operation scheduling.

Author Contributions: Conceptualization, Q.Z. and J.L.; methodology, Q.Z. and L.W.; software, W.K.; validation, W.K., L.W. and Z.W.; formal analysis, J.L.; investigation, W.K.; resources, Q.Z.; data curation, W.K.; writing—original draft preparation, Z.W.; writing—review and editing, Q.Z.; visualization, W.K.; supervision, Q.Z.; project administration, Q.Z.; funding acquisition, J.L. All authors have read and agreed to the published version of the manuscript.

Data Availability Statement: The original contributions presented in this study are included in this article, further inquiries can be directed to the corresponding author.

Conflicts of Interest: Qipei Zhang, Jixiang Lu, Wenteng Kuang, Lin Wu, and Zhaohui Wang are employees of NARI Technology Co., Ltd. This paper reflects the views of the scientists, and not the company.

Appendix A

Table A1. SVM prediction results without considering EV charging load prediction components.

Nodes/Parameters	Error	Average Error
1	2.75%	
2	2.03%	
3	3.17%	
4	3.35%	
5	2.15%	
6	2.25%	
7	3.25%	
8	3.01%	
9	3.77%	
10	2.08%	
11	2.17%	
12	2.06%	
13	2.24%	
14	3.57%	
15	2.74%	
16	2.22%	
17	2.13%	2.72%
18	1.15%	
19	2.24%	
20	2.07%	
21	2.94%	
22	3.11%	
23	4.03%	
24	3.17%	
25	2.56%	
26	3.51%	
27	2.76%	
28	3.25%	
29	3.31%	
30	4.00%	
31	2.15%	
32	2.17%	

Appendix B

Table A2. SVM prediction results considering EV charging load prediction components.

Nodes/Parameters	Error	Average Error
1	1.15%	
2	1.27%	
3	1.29%	
4	1.57%	
5	1.97%	
6	1.22%	
7	1.57%	
8	1.69%	
9	2.01%	
10	1.99%	
11	1.11%	
12	1.59%	
13	1.35%	
14	1.49%	
15	1.44%	
16	1.53%	
17	1.22%	1.65%
18	1.74%	
19	1.82%	
20	1.93%	
21	2.00%	
22	1.73%	
23	1.21%	
24	1.42%	
25	1.51%	
26	1.32%	
27	1.03%	
28	0.05%	
29	0.95%	
30	1.35%	
31	1.13%	
32	1.10%	

Appendix C

Table A3. Specific driving data for some EVs.

EV Number	EV Type	EV Initial Position	EV Destination	EV Departure Time (h)	EV Return Time (h)	EV SOC Capacity	EV Initial SOC (%)	EV Velocity (km/h)
1	3 (public EV)	10	9	7.73	20	219.77	0.27	40.58
2	1 (private EV)	27	12	7.98	18.75	211.18	0.29	40.05
3	3	8	15	6.62	18.96	201.64	0.26	39.91
4	1	26	15	7.16	18.94	220.87	0.35	40.25
5	3	3	18	6.2	18.31	266.55	0.33	38.26
6	3	27	19	7.76	19.43	279.62	0.31	39.15
7	3	13	10	6.64	18.71	231.02	0.27	39.34
8	2 (taxi EV)	19	12	7.39	19.28	207.2	0.27	42.36
9	3	4	9	7.83	18.29	212.4	0.39	40.09
10	3	6	19	7.26	18.2	203.74	0.38	40.69
11	3	28	22	6.44	18.95	294.47	0.2	38.88
12	2	10	23	7.46	19.9	283.61	0.35	36.71
13	2	31	20	7.42	18.27	256.47	0.22	40.68
14	3	1	16	7.57	19.35	234.14	0.19	39.66
15	2	31	1	6.74	19.64	238.36	0.32	40.02

Table A3. *Cont.*

EV Number	EV Type	EV Initial Position	EV Destination	EV Departure Time (h)	EV Return Time (h)	EV SOC Capacity	EV Initial SOC (%)	EV Velocity (km/h)
16	2	31	32	6.71	19.34	281.73	0.29	39.41
17	3	9	31	6.24	19.71	246.51	0.42	41.9
18	2	22	15	6.24	19.99	227.16	0.48	39.31
19	3	20	24	7.63	18.56	229.4	0.38	40.74
20	1	20	32	7.12	18.17	256.94	0.38	39.55
21	2	11	31	7.93	19.38	210.83	0.23	39.3
22	1	4	1	7.7	18.1	239.94	0.25	40.13
23	2	22	8	6.31	19.32	261.14	0.44	40.45
24	2	21	2	7.05	18.67	251.71	0.36	39.26
996	2	11	15	6.49	18.29	261.48	0.35	39.54
997	1	23	27	6.5	19.5	265.19	0.23	39.76
998	3	16	7	6.11	18.5	200.76	0.43	40.05
999	2	26	18	6.53	18.02	241.12	0.15	40.04
1000	2	18	31	7.9	19.34	280.61	0.32	40.1

References

1. Yao, M.; Da, D.; Lu, X.; Wang, Y. A Review of Capacity Allocation and Control Strategies for Electric Vehicle Charging Stations with Integrated Photovoltaic and Energy Storage Systems. *World Electr. Veh. J.* **2024**, *15*, 101. [CrossRef]
2. Zhu, B.; Bao, C.; Yao, M.; Qi, Z. Dynamic Programming of Electric Vehicle Reservation Charging and Battery Preheating Strategies Considering Time-of-Use Electricity Price. *World Electr. Veh. J.* **2024**, *15*, 90. [CrossRef]
3. Vishnuram, P.; Alagarsamy, S. Grid Integration for Electric Vehicles: A Realistic Strategy for Environmentally Friendly Mobility and Renewable Power. *World Electr. Veh. J.* **2024**, *15*, 70. [CrossRef]
4. Li, X.; Li, C.; Jia, C. Electric Vehicle and Photovoltaic Power Scenario Generation under Extreme High-Temperature Weather. *World Electr. Veh. J.* **2024**, *15*, 11. [CrossRef]
5. Zhang, Y.; Meng, X.; Shotorbani, A.M.; Wang, L. Minimization of AC-DC grid transmission loss and DC voltage deviation using adaptive droop control and improved AC-DC power flow algorithm. *IEEE Trans. Power Syst.* **2020**, *36*, 744–756. [CrossRef]
6. Hu, Q.; Han, R.; Quan, X.; Wu, Z.; Tang, C.; Li, W.; Wang, W. Grid-Forming Inverter Enabled Virtual Power Plants with Inertia Support Capability. *IEEE Trans. Smart Grid* **2022**, *13*, 4134–4143. [CrossRef]
7. Menos-Aikateriniadis, C.; Sykiotis, S.; Georgilakis, P.S. Unlocking the potential of smart EV charging: A user-oriented control system based on Deep Reinforcement Learning. *Electr. Power Syst. Res.* **2024**, *230*, 110255. [CrossRef]
8. Khan, W.; Somers, W.; Walker, S.; de Bont, K.; Van der Velden, J.; Zeiler, W. Comparison of electric vehicle load forecasting across different spatial levels with incorporated uncertainty estimation. *Energy* **2023**, *283*, 129213. [CrossRef]
9. Zhang, Y.; Mohammadpour Shotorbani, A.; Wang, L.; Mohammadi-Ivatloo, B. Enhanced PI control and adaptive gain tuning schemes for distributed secondary control of an islanded microgrid. *IET Renew. Power Gener.* **2021**, *15*, 854–864. [CrossRef]
10. Liu, J.; Lin, G.; Rehtanz, C.; Huang, S.; Zhou, Y.; Li, Y. Data-driven intelligent EV charging operating with limited chargers considering the charging demand forecasting. *Int. J. Electr. Power Energy Syst.* **2022**, *141*, 108218. [CrossRef]
11. Yiyao, Y.; Yugong, L.; Tao, Z.; Keqiang, L. Optimal charging route recommendation method based on transportation and distribution information. *Proc. CSEE* **2015**, *35*, 310–318.
12. Luo, Y.; Zhu, T.; Wan, S.; Zhang, S.; Li, K. Optimal charging scheduling for large- scale EV (electric vehicle) deployment based on the interaction of the smart-grid and intelligent- transport systems. *Energy* **2016**, *97*, 359368. [CrossRef]
13. Shao, Y.; Mu, Y.; Yu, X.; Dong, X.; Jia, H.; Wu, J.; Zeng, Y. A spatialtemporal charging load forecast and impact analysis method for distribution network using EVs- trafficdistribution model. *Proc. CSEE* **2017**, *37*, 5207–5219.
14. El-Azab, H.A.I.; Swief, R.A.; El-Amary, N.H.; Temraz, H.K. Seasonal electric vehicle forecasting model based on machine learning and deep learning techniques. *Energy AI* **2023**, *14*, 100285. [CrossRef]
15. Liao, B.; Gao, Z.; Tang, J.; Wu, Y.; Cheng, J.; Hou, J. Research on centralized direction protection of active distribution network based on graph theory. *Smart Power* **2019**, *47*, 55–62.
16. Junhua, Z.; Fushuan, W.; Aimin, Y.; Jianbo, X. Impacts of electric vehicles on power systems as well as the associated dispatching and control problem. *Autom. Electr. Power Syst.* **2011**, *35*, 210.
17. Zhang, Y.; Qian, W.; Ye, Y.; Li, Y.; Tang, Y.; Long, Y.; Duan, M. A novel non-intrusive load monitoring method based on ResNet-seq2seq networks for energy disaggregation of distributed energy resources integrated with residential houses. *Appl. Energy* **2023**, *349*, 121703. [CrossRef]
18. Zhang, Y.; Shotorbani, A.M.; Wang, L.; Mohammadi-Ivatloo, B. Distributed secondary control of a microgrid with a generalized PI finite-time controller. *IEEE Open Access J. Power Energy* **2021**, *8*, 57–67. [CrossRef]

19. Ranceva, J.; Ušpalytė-Vitkūnienė, R. Specifics of Creating a Public Transport Demand Model for Low-Density Regions: Lithuanian Case. *Sustainability* **2024**, *16*, 1412. [CrossRef]

20. Sarda, J.; Patel, H.; Popat, Y.; Hui, K.L.; Sain, M. Review of Management System and State-of-Charge Estimation Methods for Electric Vehicles. *World Electr. Veh. J.* **2023**, *14*, 325. [CrossRef]

21. Peng, Q.; Zheng, Z.; Hu, H. Defect Prediction for Capacitive Equipment in Power System. *Appl. Sci.* **2024**, *14*, 1968. [CrossRef]

22. Zhao, Y.; Jiang, Z.; Chen, X.; Liu, P.; Peng, T.; Shu, Z. Toward environmental sustainability: Data-driven analysis of energy use patterns and load profiles for urban electric vehicle fleets. *Energy* **2023**, *285*, 129465. [CrossRef]

23. Zhang, Y.; Meng, X.; Malik, A.; Wang, L. The use of analytical converter loss formula to eliminate DC slack/droop bus iteration in sequential AC-DC power flow algorithm. *Int. J. Electr. Power Energy Syst.* **2022**, *137*, 107596. [CrossRef]

24. Zhou, S.; Zang, X.; Yang, J.; Chen, W.; Li, J.; Chen, S. Modelling the Coupling Relationship between Urban Road Spatial Structure and Traffic Flow. *Sustainability* **2023**, *15*, 11142. [CrossRef]

25. Zheng, W.; Zhou, X.; Bai, C.; Zhou, D.; Fu, P. Adaptation of Deep Network in Transfer Learning for Estimating State of Health in Electric Vehicles during Operation. *Batteries* **2023**, *9*, 547. [CrossRef]

26. Global Modeling and Assimilation Office (GMAO). MERRA-2 tavgU_2d_flx_Nx: 2d, Diurnal, Time-Averaged, Single-Level, Assimilation, Surface Flux Diagnostics V5.12.4, Greenbelt, MD, USA, Goddard Earth Sciences Data and Information Services Center (GES DISC). 2015. Available online: https://disc.gsfc.nasa.gov/datasets/M2TUNXFLX_5.12.4/summary (accessed on 25 February 2024).

27. Rassaei, F.; Soh, W.-S.; Chua, K.-C. Demand Response for Residential Electric Vehicles with Random Usage Patterns in Smart Grids. *IEEE Trans. Sustain. Energy* **2015**, *6*, 1367–1376. [CrossRef]

28. Azimi Nasab, M.; Zand, M.; Padmanaban, S.; Khan, B. Simultaneous Long-Term Planning of Flexible Electric Vehicle Photovoltaic Charging Stations in Terms of Load Response and Technical and Economic Indicators. *World Electr. Veh. J.* **2021**, *12*, 190. [CrossRef]